Journal of Bioenergetics and Biomembranes, Vol. 30, No. 6, 1998

Fast- and Slow-Gating Modes of the Sodium Channel Are Altered by a Paramyotonia Congenita-Linked Mutation

Oscar Moran,[1,2] Raffaella Melani,[1] Mario Nizzari,[1] and Franco Conti[1]

Received August 4, 1998; accepted October 13, 1998

We have studied the expression in frog oocytes of the α subunit of the rat skeletal muscle sodium channel mutation T1306M, homologous to the mutation T1313M of the human isoform that causes the muscular hereditary disease paramyotonia congenita. Wild-type (WT) channels show a bimodal behavior, with two gating modes characterized by inactivation time constants that differ at least by one order of magnitude and with voltage dependencies shifted by +27 mV in the slow mode (M2) relative to the fast (M1) mode. In the myopathy-linked mutant the propensity of the channel for the mode M2 is increased fourfold and the kinetics and voltage dependence of inactivation in both modes are altered. In mode M1, the onset of inactivation is faster and the recovery from inactivation is slower whereas both processes are slowed in mode M2. The half-inactivation potential of both modes is shifted by the mutation to positive potentials. Coexpression of β subunit causes a threefold reduction of the M2 propensity of both WT and T1306M channels, with small changes in the voltage dependency and kinetic properties of inactivation. All the changes are consistent with the hyperexcitability of the muscle fibers observed in patients affected by potassium-aggrevated myotonia (PAM).

KEY WORDS: Sodium channel; paramyotonia congenita; inactivation; modal gating; oocytes; hereditary disease.

INTRODUCTION

Anomalies in the adult skeletal muscle sodium channels responsible for the initial phase of the action potential, can have important consequences for muscle physiology and cause pathological conditions (Barchi, 1995; Cannon, 1996). This is exemplified by a group of autosomal dominant hereditary muscle diseases, including paramyotonia congenita (PC), potassium-aggravated myotonia (PAM) and hyperkalemic periodic paralysis (HyPP). To date, 21 different point mutations of the SCN4A gene, localized in chromosome 17q (23.1 to 25.2) and coding for the human skeletal muscle sodium channel α subunit (hSkM1), have been linked with muscle sodium channelopathies (Bulman, 1997). The pathology of the mutant phenotypes has been most commonly attributed to defects in the mechanism of inactivation, causing hyperexcitability of sarcolemma with consequent myotonic and possible paralytic episodes in patients (Cannon, 1996; Hoffman *et al.*, 1995).

Because the functional properties of the mutant channels are difficult to measure in native muscle fibers, many groups have studied the heterologous expression of the hSkM1 α subunit in cDNA-transfected mammalian cells or in cRNA-injected frog oocytes. The characteristics of the sodium currents expressed by mammalian cells transfected by the SkM1 α subunit closely resemble those of native muscle fibers, probably because the cells are able to endogenously express other molecular components, in particular, the sodium channel β_1 subunit (Mitrovic *et al.*, 1994) that seems to modulate the gating properties of the channel. Although differently, the channels expressed by frog oocytes injected with the cRNA of the sole α subunit mediate an abnormally high percent-

[1] Istituto di Cibernetica e Biofisica, CNR, Via De Marini, 6, I-16149 Genova, Italy.
[2] Author to whom correspondence should be sent.

0145-479X/98/1200-0579$15.00/0

age of slowly inactivating sodium currents (Auld *et al.*, 1988; Moorman *et al.*, 1990; Moran *et al.*, 1998a; Trimmer *et al.*, 1989; Zhou *et al.*, 1991) that are substantially reduced by coexpression of the β_1 subunit (Ji *et al.*, 1994; Patton *et al.*, 1994; Richmond *et al.*, 1997a; Zhou *et al.*, 1991) but are not totally absent (Cannon *et al.*, 1993b; Chang *et al.*, 1996; Patton *et al.*, 1994; Wallner*et al.*, 1993). On the other hand, exacerbation of the slow-mode behavior makes this system more appropriate for studying the intrinsic modal propensity of the main subunit of the channel. We have used the expression in frog oocytes of the α subunit alone, or the coexpression of the α and β_1 subunit of the adult rat skeletal muscle sodium channel (rSkM1, μ1), which have more than 90% identity with the human one. In this work, we compare the functional properties of the fast and slow modes of the wild-type sodium channel with those of the PAM mutant T1306M. We find that this mutation changes the voltage dependence and the kinetics of inactivation of both modes, besides increasing the propensity of α subunit channels for the slow mode. The coexpression of the β_1 subunit decreases this propensity by the same factor in WT and T1306M channels.

MATERIALS AND METHODS

Mutagenesis

The full-length cDNA coding for the rSkM1 sodium channel α subunit (Trimmer *et al.*, 1989) was subcloned into the Eco*RI* site of the high expression prokaryotic vector pGEMHE, containing the 5′UTR and the 3′UTR untranslated sequences of the bovine β-globin gene that induces a high expression in frog oocytes (Liman *et al.*, 1992). We prepared the T1306M mutation of the cytoplasmic linker between domains III and IV (corresponding to the human mutation T1313M) by site-directed mutagenesis using the QuikChange kit (Strategene) and the Pfu DNA polymerase (Kudel, 1985; Sugimoto *et al.*, 1989). Two mutagenic primers of 44 nucleotides, each complementary to the two opposite strands of the cDNA in the region to be modified, were purchased by order (Geneco, Florence). These primers are extended to the full circular plasmid containing the cDNA insert during temperature cycling by means of the Pfu DNA polymerase. The Dpn *I* endonuclease, specific for methylated DNA, was used to digest the parental DNA template. The mutations were verified by sequencing 400 bp's of a region including the mutagenic point by dideoxynucleotides methods (Sanger *et al.*, 1977).

cRNA Preparation and Expression

The plasmids containing the wild-type (WT) α subunit cDNA or the T1306M mutation were linearized with Nhe *I*. Plasmids containing the cDNA coding the rat brain sodium channel β_1 subunit (psPNa-beta, generous gift of K. Imoto) were linearized with Eco*RI*. *In vitro* transcription of the cDNA was done with T7 polymerase at 37°C for 2 h, using the capped mMessage mMachine kit (Ambion). After digesting the DNA template with DNase I, cRNA was precipitated in LiCl. The pellet was washed with 70% ethanol, resuspended in DEPC-treated water, and stored at −80°C for further use.

Oocytes were surgically extracted from anesthetized *Xenopus laevis*, and freed from the follicular membrane by enzymatic treatment of the frog ovarian tissue with a Ca–Mg-free Bart's solution containing 1 mg/ml of collagenase A (Sigma) for 1.5 to 2 h at room temperature. Stage IV or stage V oocytes were injected with 50 nl of 125 to 250 ng/μl solution of cRNA coding the sodium channel α subunit in DEPC-water, and incubated 4–7 days in Bart's solution at 18°C (Stühmer, 1992). In some experiments, the β_1 subunit (100 μg/μl) was coinjected together with the α subunit.

Electrophysiological Recording

About 20 minutes before beginning of electrophysiological measurements, the oocytes were made to shrink by exposure to hypertonic solution and mechanically deprived of the viteline membrane using fine forceps. They were then transferred to the recording chamber where they were allowed to retrieve their normal volume in the final bathing solution that had the following composition (in m*M*): KCl 120, Tris-Cl 20, EGTA 5; pH 7.4.

Sodium currents were measured from membrane macropatches in the cell-attached configuration (Hamill *et al.*, 1981; Stühmer, 1992) using an Axopatch-200B patch–clamp amplifier (Axon Instruments). Aluminum-silicate glass micropipettes (Hilgemberg) were coated with silicone rubber and fire-polished to a tip diameter yielding a resistance of 0.6 to 1.2 MΩ in the working solutions. The pipette was filled with normal

frog Ringer (in m*M*: NaCl 115, KCl 2.5, $CaCl_2$ 1.8, HEPES 10; pH = 7.4). Because of the high potassium concentration of the bath solution, the cell membrane potential was 0 ± 2 mV. Therefore, the membrane patch potential, *V*, was estimated to be just opposite to the pipette potential. The current to voltage conversion at the output of the patch-clamp amplifier was filtered with the built-in low-pass four-pole Bessel filter set at a cut-off frequency of 5 kHz and sampled at 20 kHz. The membrane patch was kept at a holding potential of −120 mV during measurements. Voltage stimulation and data acquisition were done by 16 bit D-A and A-D converters (ITC-16, Instrutech), controlled by a Macintosh microcomputer, using Pulse software (Heka Electronik). The linear components of the responses were measured with subthreshold stimulations and digitally subtracted. All measurements were done at a controlled temperature of 15 ± 0.5°C.

Data Analysis

Data were analyzed with a Macintosh microcomputer using PulseFit (Heka Electronik) and custom software developed in the Igor environment (Wavemetrics). Statistical comparisons were done with Student's *t* test, and statistical significance was defined by $p < 0.05$. The results were expressed as mean ± sem. Theoretical curve fitting was made by a simplex method and the error bars in the figures represent the standard error of the mean. Data were obtained from four different batches of oocytes for WT and three different batches for mutant channels.

RESULTS

Modal Propensity of WT and T1306M Channels

Both WT and mutant cRNA's expressed sodium currents in oocytes, although the mutant yielded, on average, smaller current amplitudes (Fig. 1). The maximum peak current measured within 3–4 minutes after having obtained the giga-seal was between 130 pA and 3 nA for WT. Lower expression levels, between 100 and 800 pA ($p < 0.05$) were found for mutant T1306M. In all cases, the current increased during an experiment on a stable patch up to two- to three-fold after 20–35 min from patch isolation.

In the oocyte system, the current mediated by the rSkM1 α subunit channels is characterized by a rapid

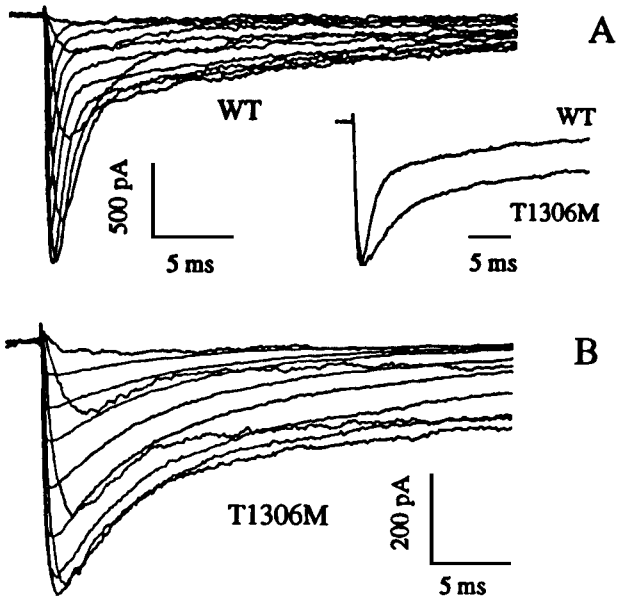

Fig. 1. Sodium currents expressed in *Xenopus* oocytes microinjected with cRNA coding WT (A) and T1306M (B) rSkM1 sodium channel α subunits. Currents were elicited by depolarizing pulses from a holding potential of −120 mV to test potentials increasing from −50 to 50 mV in 10 mV steps. The inactivation of the currents is characterized by two time constants. The inset shows the direct comparison of WT and T1306M currents, scaled to the same peak amplitude, for a step of voltage near the half-activation potential. Notice the strong increase of the relative amplitude of slower component in the T1306M current.

increase followed by a biphasic inactivation, as shown in Figs. 1 and 2 (Ji *et al.*, 1994; Moorman *et al.*, 1990; Moran *et al.*, 1998a, b; Zhou *et al.*, 1991). The decay of the current can be well fitted with a double-exponential function as:

$$I(t) = a_1 e^{(-t/\tau_1)} + a_2 e^{(-t/\tau^2)},$$

where τ_1 and τ_2 indicate the fast and slow time constants, differing by about one order of magnitude (Fig. 2). It has been proposed that the two components are due to the separate contributions of a mixed population of channels that are either in a fast or in a slow mode of inactivation at the time of the stimulus. In the fast-inactivating mode, which we shall call M1, the channels most likely open only once and briefly during the depolarizing stimulus, while in the slow mode, called M2, channels have late reopenings during the sweep (Moorman *et al.*, 1990; Zhou *et al.*, 1991). The ratio of the two amplitudes a_1 and a_2 is fairly independent of the depolarizing voltage, indicating that the voltage dependence of activation is roughly similar for the two

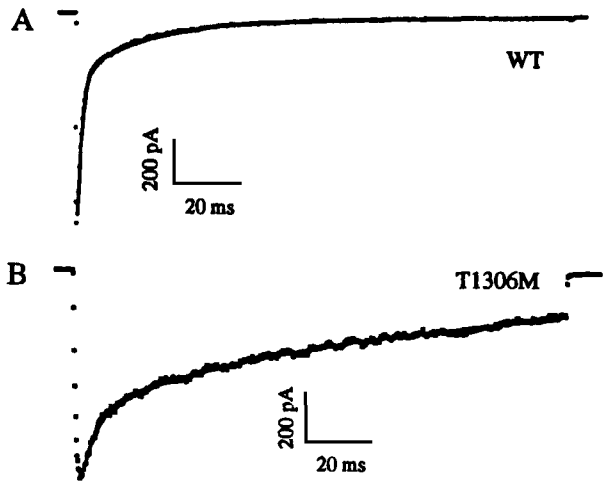

Fig. 2. WT (A) and T1306M (B) currents elicited by a 150-ms depolarizing pulse from a holding potential of −120 mV to a test potential of ~20 mV more positive than the half-activation potential. The falling phase of the current is fitted with a double-exponential function, yielding τ_1 = 1.2 ms, τ_2 = 23 ms, and P_{M2} = 11% for WT channels, and τ_1 = 5 ms, τ_2 = 67 ms, and P_{M2} = 47% for T1306M channels.

gating modes (Hayward *et al.*, 1996; Moran *et al.*, 1998a, b).

As shown in Figs. 1A and 2A, and in agreement with several previous reports (Ji *et al.*, 1994; Moorman *et al.*, 1990; Moran *et al.*, 1998a, b; Trimmer *et al.*, 1989), the M2 component of the currents expressed by α subunits in oocytes is quite substantial, in contrast with the heterologous expression of muscle sodium channels in mammalian cells where the contribution of mode M2 is estimated less than 2% (Ukomadu *et al.*, 1992). Our present studies show that the M2 contribution is even much larger for channels expressed in oocytes injected with the cRNA of the α subunit mutant T1306M. This is illustrated in the inset of Fig. 1 by the comparison of the records of WT and T1306M responses scaled to the same peak value: the larger slow component of the mutant channel results in a much larger late current for pulses of 30-ms duration.

To quantify the propensity of the channels to gate in the mode M2, we defined the parameter $P_{M2} = a_2/(a_1 + a_2)$, as a measure of the probability of finding the channels in mode M2 at the time of the test stimulus. P_{M2} was estimated from the double-exponential fit of the decaying phase of the sodium currents evoked by 30 to 150 ms depolarization to voltages between −20 and +30 mV. We found that P_{M2} was fairly independent of voltage in this range. A systematic decrease of P_{M2}, in many cases down to about 30% of the initial estimates, was instead observed during the first 20 min from patch isolation (Moran *et al.*, 1998a; Richmond *et al.*, 1997a). However, this trend was common to both measurements with WT and mutant channels and does not affect much the relative comparison of the P_{M2} estimates for the two phenotypes. The early values of P_{M2} (within 4 min from patch isolation) were significantly larger for mutant T1306M (44 ± 15%, n = 10), compared to WT (10.4 ± 6%; n = 15). Interestingly, coexpression of the β_1 subunits reduced P_{M2} in both WT and T1306M channels by about the same factor of 3, respectively, to 3.5 ± 0.5% (n = 21) and 13 ± 2% (n = 8) (data not shown), suggesting that the main effect of the α–β_1 interaction is a reduction of the propensity of the channels for mode M2 that is largely unaffected by the mutation. This is consistent with the observations that in preparations showing smaller values of P_{M2}, as in mammalian cells transfected with rat or human SkM1 channels (Hayward *et al.*, 1996, 1997) or in biopsies of patients with PC (Tahmoush *et al.*, 1994), the mutant phenotype is also characterized by an increase of the slowly inactivating currents.

A feature of patch recording that disturbs the measurement of the voltage dependencies of activation and inactivation parameters is the fact that in most experiments a negative shift of 5 to 30 mV in the activation curves occurs gradually, within 20–40 min from the isolation of a single patch. Such artifact has been recently suggested to arise from the disturbance of the channel–cytoskeleton interactions caused by the local mechanical stress associated with the patch isolation (Shcherbatko and Brehm 1998), and similar changes have been reported from recordings from HEK 293 cells permanently transfected with rSkM1 channels (Cummins and Sigworth, 1996) or from cardiac muscle fibers (Wend *et al.*, 1992). In order to cope with these variations, likely arising from changes of surface-potential offsets, we found it very useful to express the voltage dependencies in term of a relative potential, $V_{rel} = V - V_{1/2}$, where V is the controlled voltage and $V_{1/2}$ is the potential at which the peak conductances reach 50% of their maximum value. In agreement with previous reports (Ji *et al.*, 1994; Moran *et al.*, 1998a, b, c), we found no significant differences between the activation curves of mode M1 and mode M2, when measured at approximately the same time by dissecting the modes, as discussed later (Fig. 3A). Therefore, we do not expect that $V_{1/2}$ changes with P_{M2}. $V_{1/2}$ was measured periodically and systematically during each experiment, and, when necessary, was estimated by interpolation of experiments at earlier and

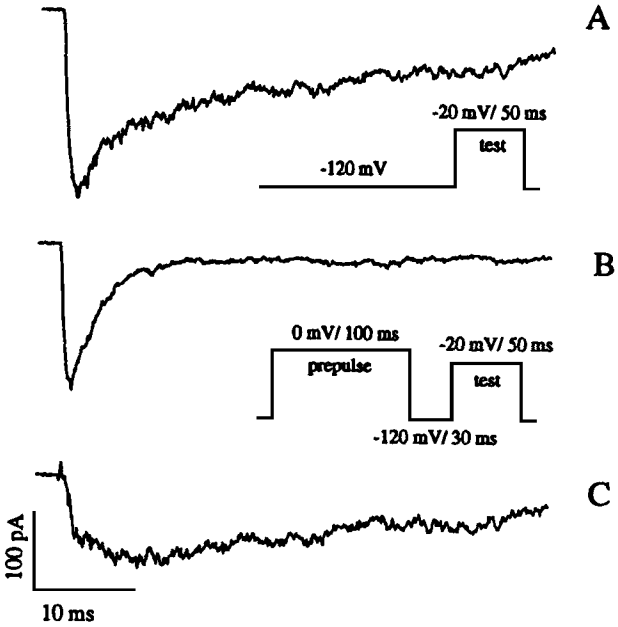

Fig. 3. Dissection of the two gating modes in the current expressed by T1306M channels. (A) The current recorded using the protocol indicated in the figure shows a biphasic inactivation. (B) When the test pulse is preceded by a conditioning prepulse and by a repolarization period, the test current shows a single-exponential decay and is due only to channels gating in mode M1, that have recovered from inactivation almost completely in ~30 ms, whereas M2 currents that have a 20-fold larger recovery time are still practically undetectable. (C) The M2 contribution is obtained by subtraction of trace in (B) from the trace (A).

later times. The absolute values of $V_{1/2}$ could vary in our measurements between -7 and -40 mV in 25 min. When expressed as a function of V_{rel}, voltage-dependent data obtained at different times during an experiment were fully consistent and gave much more confidence in the comparison of the results from different experiments.

Inactivation Kinetics

In order to evaluate the kinetics of inactivation, we have systematically fitted the decaying phase of the currents evoked by 30-ms or 50-ms pulses to membrane potentials between -30 to 30 mV (corresponding to V_{rel} approximately in the range of $-10 + 50$ mV) with a double-exponential function, as described above (see Fig. 2). In some cases, in particular at low membrane potentials, when the fast component of the current was too small or not differentiated kinetically enough to be easily dissected by computer fit, we used a conditioned stimulation protocol (Moran *et al.*, 1998a) to separate the contributions of the two gating modes, as shown in Fig. 3. The test pulse is preceded by a conditioning prepulse to 0 mV for 100 ms and by a brief repolarizing pulse (30 ms at -120 mV). While the conditioning prepulse causes the full inactivation of all channels, the repolarization period is long enough to remove the inactivation of the channels gating in mode M1 but largely insufficient for the retrieval from the inactivated state of M2 channels. Therefore, the test response is exclusively characterized by the properties of channels gating in mode M1. The conditioned responses allowed fairly accurate estimates of the M1 inactivation time constant, τ_1. The nonconditioned response to the same test pulse was then fitted with a double-exponential, holding the fast time constant fixed to the value just determined. The reliability of this strategy was checked for test voltages for which the nonconditioned records allowed a clear dissection of the components by a double-exponential fit. The τ_1 estimates obtained from single-exponential fits of the conditioned record or from the double-exponential fit of the nonconditioned one were statistically indistinguishable.

To evaluate the time constants of inactivation for values of V_{rel} between -20 and -60 mV, we measured the current evoked by a test pulse to $V \geq -10$ mV, after a conditioning prepulse of variable duration (0.5–500 ms) to the desired voltage. The plot of peak response against the duration of the conditioning prepulse was fitted with a double-exponential function, yielding the time constant, τ_1 and τ_2, respectively, of inactivation of mode M1 and mode M2 at the prepulse potential.

For membrane potentials corresponding to V_{rel} in the range of -50 to -80 mV, inactivation was characterized by studying recovery kinetics. All channels were inactivated by a conditioning pulse of 150 ms to 0 mV and allowed to recover from inactivation for a period of variable duration (1–500 ms) to the desired potential. The peak response to a test pulse applied at the end of this period was plotted against the duration of the recovery interval and fitted with a double-exponential function, with time constants τ_1 and τ_2. For some experiments, we also analyzed the recovery of the average current during the last 7.5 ms of the 30-ms test pulse. In agreement with the fact that the late current is due almost exclusively to channels gating in mode M2, these data were well fitted by a single exponential, with a time constant close to the value of τ_2 obtained from the fit of the peak currents.

Since stimulation protocols were prepared for fixed values of V, whereas the estimates of $V_{1/2}$ changed with time and differed from experiment to experiment, the data obtained correspond to scattered values of V_{rel}. For this reason they were grouped in 20-mV bins for convenience of presentation. The overall summary of τ_1 and τ_2 measurements for WT and T1306M channels is presented in Fig. 4A and B, where ± sem for V_{rel} and for the measured parameter in the ordinate are represented by horizontal and vertical bars, respectively.

Contrary to our previous observation on the PAM mutant S798F (Moran *et al.*, 1998b), for which the most significant changes in inactivation properties were found in the time constants of mode M2, the PC mutant T1306M studied here showed very large differences with respect to WT also in the inactivation time constant of mode M1. In general, mode M1 of mutant T1306M is characterized by a faster recovery from inactivation and by slower kinetics for the onset of inactivation, whose time constant is almost voltage independent for $V_{rel} > 0$ mV. The maximum of the τ_1-V_{rel} plot that clearly characterizes WT data is almost unappreciable in the mutant and seems shifted by more than 20 mV to more positive potentials. The estimates of τ_1 at $V_{rel} \leq -30$ mV are 5 to 15 times smaller for T1306M than for WT (see Table I). While in WT channels τ_1 decreases with voltage (from 14 ms at $V_{rel} = -30$ mV to 0.3 ms at $V_{rel} = 70$ mV), for more positive potentials in mutant T1306M, it seems to reach a plateau of 4.5 ms at $V_{rel} > -30$ mV (Fig. 4A). Similar results have been reported from experiments with oocytes expressing the α subunit of the WT human sodium channel and the equivalent mutation (T1313M) (Richmond *et al.*, 1997a), while mode M2 was strongly depressed by coinjection of the β_1 subunit cRNA. In addition, the expression of rat or human WT or mutant channels in mammalian cells, where mode M2 is endogenously depressed, leads to the same con-

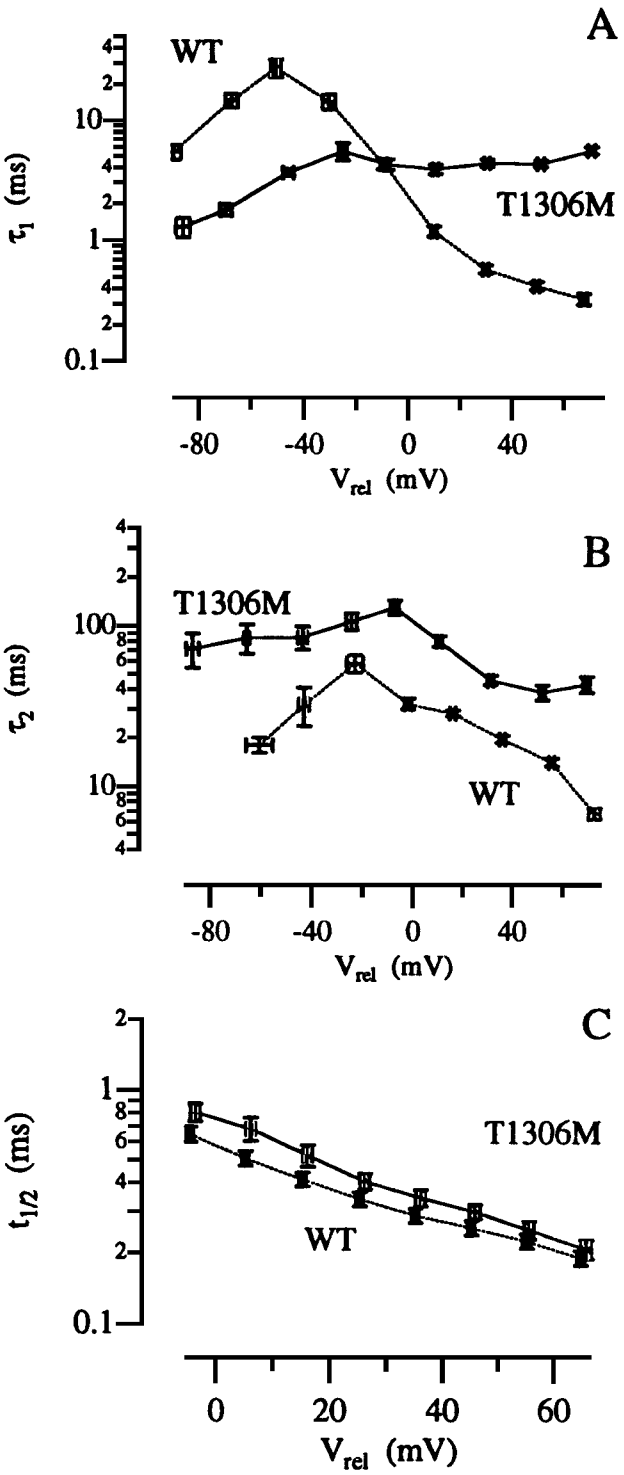

Fig. 4. Voltage dependence of the inactivation and activation kinetics of WT (broken lines) and T1306M (continuous lines) currents. Voltage is expressed as deviation from the half-activation potential, V_{rel}. (A) The inactivation time constant of mode M1, τ_1, is larger for the mutant channels at positive potentials, and smaller at negative potential. (B) The inactivation time constant of mode M2, τ_2, is larger for T1306M than for WT at all potentials. (C) The time to half of the maximum current, $t_{1/2}$, is systematically slightly longer for T1306M. This may be an indirect effect, quantitatively expected as a consequence of the slower inactivation kinetics of T1306M for $V_{rel} > -10$ mV.

Table I. Propensity of Mode M2 and Inactivation Time Constants of Mode M1 and Mode M2[a]

		WT		T1306M	
	V_{rel}(mV)	α	α + β	α	α + β
P_{M2}[b]		0.10 ± 0.06	0.035 ± 0.005	0.44 ± 0.15	0.13 ± 0.02
		n = 15	n = 21	n = 10	n = 8
τ_1[c] (ms)	−50	27.7 ± 4.6	—	3.7 ± 1.0	—
		n = 9		n = 9	
	−5	4.3 ± 0.4	1.5 ± 0.2	4.3 ± 0.5	3.1 ± 0.4
		n = 28	n = 20	n = 31	n = 8
	50	0.42 ± 0.03	0.36 ± 0.02	4.3 ± 0.3	3.2 ± 0.3
		n = 26	n = 18	n = 21	n = 8
τ_2[d] (ms)	−40	32.2 ± 8.6	—	84.5 ± 14.1	—
		n = 5		n = 5	
	−5	32.2 ± 2.4	20.2 ± 1.8	130.6 ± 13.6	163 ± 20.8
		n = 16	n = 19	n = 17	n = 7
		14.0 ± 0.8	14.0 ± 1.5	32.2 ± 4.1	64.2 ± 20.8
		n = 26	n = 18	n = 20	n = 7

[a] Measured from oocytes expressing WT or T1306M mutant of the sodium channel α subunit alone or in association with the β subunit.
[b] Propensity of gating in mode M2.
[c] Mode M1 inactivation time constant.
[d] Mode M2 inactivation time constant.

clusion (Hayward *et al.*, 1996; Yang *et al.*, 1994). A faster recovery from inactivation and slower and less voltage-dependent kinetics for the onset of M1 inactivation have also been described for the expression in mammalian cells of other mutations of the muscle sodium channel (L1433R, R1448C/H, F1473S) that produce the same disease (Chahine *et al.*, 1994; Ji *et al.*, 1996; Mitrovic *et al.*, 1996). In our experiments the coexpression of the β_1 subunit produces a slight decrease of both inactivation time constants at large depolarizations and a more substantial decrease in WT around $V_{1/2}$ potentials (see Table I). These observations are consistent with a slight negative shift of the voltage dependence of M1 inactivation reported by other authors as an effect of the β_1 coexpression (Cannon *et al.*, 1993b; Isom *et al.*, 1995; Makita *et al.*, 1994; Wallner *et al.*, 1993). The larger effect for WT channels at $V_{rel} = -5$ mV is expected according to the steeper slope of the voltage dependence of WT data in this region where the mutant data are fairly constant.

The M2 inactivation time constant of mutant T1306M is characterized by larger values and by a generally shallower voltage dependence. The τ_2 values for the mutant are two- to fourfold larger than those of WT at any potential (see Table I) and the peak of the τ_2-V_{rel} plot is much less pronounced and shifted about 10 mV to more positive potentials. The reduction in the voltage dependence of τ_2 is particularly evident for $V_{rel} < -5$ mV where the τ_2 of the mutant reaches a maximum. For larger values of V_{rel}, our τ_2 estimates for T1306M decrease first with a slope similar to that of WT, then tend to acquire a constant plateau for $V_{rel} \geq 20$ mV, where WT data show still a roughly twofold decrease per 10 mV increase of V_{rel}(Fig. 4B).

Activation Kinetics

A rough characterization of the activation kinetics of WT and T1306M channels was obtained by measuring the time, $t_{1/2}$, needed for the current response to a step depolarization to reach one-half of its peak amplitude. Data for V_{rel} between 0 and 70 mV, grouped in 10-mV bins, are shown in Fig. 4C. In WT channels, $t_{1/2}$ decreased with V_{rel} in the whole explored range, with a fairly exponential decay from 0.51 ± 0.04 ms (n = 15) at V_{rel} = 5 mV to 0.18 ± 0.01 ms (n = 11) at V_{rel} = 70 mV. The PC mutant showed slightly slower activation kinetics, with roughly the same voltage dependence: $t_{1/2}$ decayed from 0.68 ± 0.08 ms (n = 13) for V_{rel} = 5 mV to 0.21 ± 0.02 ms (n = 11) for V_{rel} = 70 mV. These results agree with the slight increase of $t_{1/2}$ for the same mutant expressed in mammalian cells (Hayward *et al.*, 1996; Yang *et al.*, 1994) or coexpressed in oocytes together with the β_1 subunit of the sodium channel (Richmond *et al.*, 1997a). The decrease of $t_{1/2}$ might suggest an effect of the mutation T1306M on the activation kinetics. It should be

noticed, however, that the value of $t_{1/2}$ depend both on activation and on inactivation kinetics and that a slower inactivation entrains a larger peak conductance and, consequently, a larger value of $t_{1/2}$. Therefore, we favor the hypothesis that the small increase of $t_{1/2}$ shown in Fig. 4C might very well be a consequence of the more substantial increase of τ_1, τ_2, and P_{M2}, discussed above.

Steady-State Inactivation

The voltage dependence of steady-state inactivation was measured with a double-pulse protocol. A depolarizing test pulse to $V_{rel} \geq 0$ mV was preceded by a 500-ms conditioning pulse to various membrane potentials between −120 and −30 mV. The contribution of mode M2 to the test response was estimated from the average current at the end of the test pulse (between 17 and 20 ms for WT and between 22.5 and 30 ms for T1306M). For $V_{rel} \geq 0$ mV, all the channels gating in mode M1 are fully inactivated at these times, since $\tau_1 < 4$ ms for both phenotypes (see Fig. 2B). The M1 contribution was estimated from the peak current after subtracting the estimated M2 contribution, which is obtained by extrapolating the late current to the time to peak using appropriate standard values of τ_2. Half-inactivation potentials for each mode, V_{h1} and V_{h2}, were estimated from the least-squares fit of the V_{rel} dependence of the normalized currents with Boltzmann functions (Fig. 5).

WT channels gating in the mode M1 inactivate at membrane potentials about 27 mV more negative than in mode M2: $V_{h1} = -56.3 \pm 0.8$ mV (n = 15); $V_{h2} = -29.6 \pm 1.4$ ($n = 12$) (Moran *et al.*, 1998a, b). In the mutant T1306M this difference is reduced to about 13 mV, and there is a significant positive shift of the half-inactivation potential of both modes relative to WT: $V_{h1} = -27.7 \pm 1.9$ mV ($n = 7$); $V_{h2} = -13.2 \pm 1.3$ mV ($n = 6$). A positive shift of a loosely defined mean inactivation curve has been described for the same mutation of rat or human SkM1 α subunit, expressed in mammalian cells or oocytes (Hayward *et al.*, 1996, 1997; Richmond *et al.*, 1997a; Yang *et al.*, 1994), as well as for other two PC-linked mutations, F1473S (Mitrovic *et al.*, 1996) and L1433R (Ji *et al.*, 1996). A negative shift of the steady-state inactivation curve has been reported in another PC-linked mutation, R1448C/H (Chahine *et al.*, 1994; Ji *et al.*, 1996; Richmond *et al.*, 1997a).

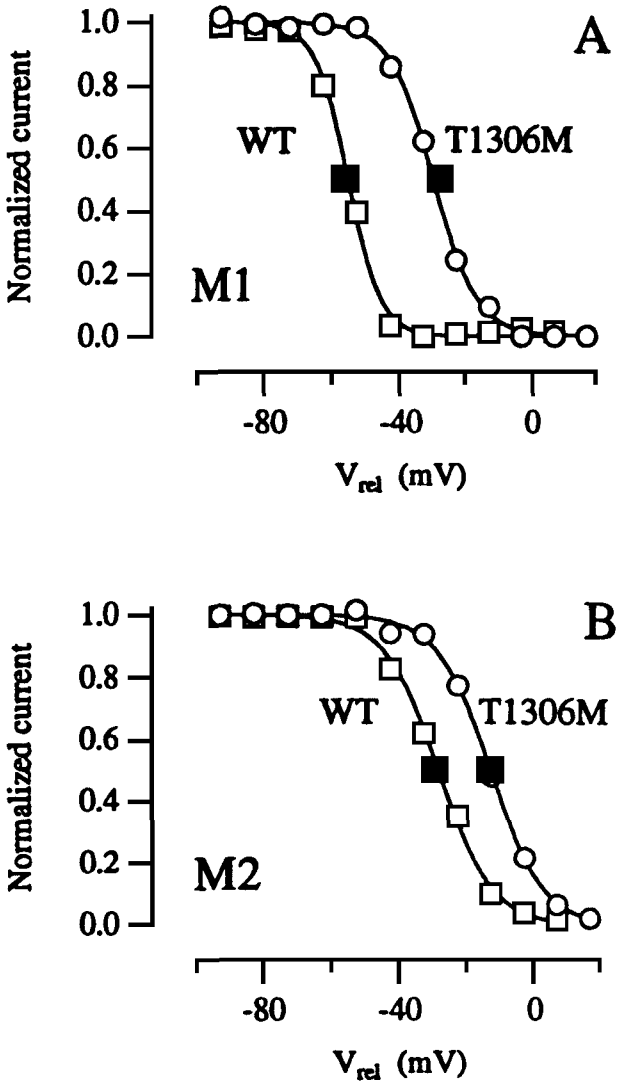

Fig. 5. Voltage dependence of the steady-state inactivation of mode M1 (A) and mode M2 (B) for WT (squares) and T1306M mutant (circles). The data are from single experiments with WT and T1306M. The continuous lines are best fits with a Boltzmann function, yielding $V_{h1} = -55.4$ mV and $V_{h2} = -28.6$ mV for WT and $V_{h1} = -29.8$ mV and $V_{h2} = -13.3$ mV for T1306M mutant. The black squares over each line indicate the mean values of half-inactivation potentials obtained form 15 experiments on WT channels and from 7 experiments on T1306M channels. Observe that the mutation causes a positive shift of the half-inactivation potential of the two modes.

DISCUSSION

When expressed in *Xenopus* oocytes, the currents mediated by the WT or the PC-linked mutation T1306M of the α subunit of rSkM1 are characterized by a double-exponential inactivation, due to the

bimodal behavior of these channels, comprising a fast inactivating mode and a slower mode, with an inactivation time constant more than tenfold larger (Ji *et al.*, 1994; Moorman *et al.*, 1990; Moran *et al.*, 1998a; Zhou *et al.*, 1991). We have chosen the heterologous expression of the rSkM1 α subunit in oocytes because the M2 mode has a much larger probability in this preparation, $P_{M2} \approx 10\%$ (Ji *et al.*, 1994; Moorman *et al.*, 1990; Moran *et al.*, 1998a; Trimmer *et al.*, 1989), whereas the same channel expressed in mammalian cells behaves more similarly to the native preparation, with $P_{M2} < 3\%$ (Ukomadu *et al.*, 1992). This is likely due primarily to the coassembly of the exogenous protein with the sodium channel β_1 subunit expressed endogenously in the human kidney cells used for transfection experiments (Mitrovic *et al.*, 1994). Indeed, the coexpression of the β_1 subunit in frog oocytes significantly reduces the propensity of α subunits for gating in the M2 mode and makes the sodium currents mediated by these channels more similar to those of the native muscle preparation (Cannon *et al.*, 1993b; Patton *et al.*, 1994; Richmond *et al.*, 1997a). However, this increases the difficulty of obtaining an accurate characterization of the M2 mode. When studying the effect of the coexpression of the β_1 subunit on the currents mediated by the WT or T1306M α-subunits, we found that P_{M2} was reduced to the same extent (~0.3) for both phenotypes, without significant changes of the voltage dependencies or the kinetics of inactivation in the two modes. We consider this observation a demonstration that our basic experimental model, i.e., the expression of the sole α subunit, is more powerful, because the exacerbation of mode M2 allows a more accurate characterization of this mode without overlooking effects expected *a priori* from the β_1 subunit interaction likely existent constitutively *in vivo*.

Our present study shows that the PC-linked mutation T1306M causes a three- to fivefold increase in the intrinsic propensity of α subunit channels to gate in the M2 mode. This result is qualitatively consistent with studies of the same mutation expressed in mammalian cells (Hayward *et al.*, 1996, 1997), and with studies of biopsies from patients carrying the homologous human mutation T1313M (Tahmoush *et al.*, 1994), although the constitutively small values of P_{M2} makes the quantitative estimate of the effect rather inaccurate.

Our results are in good agreement with previous studies of mutant T1306M mode M1 properties of α subunit channels, which indicate significant changes in kinetics and voltage-dependence of inactivation (Hayward *et al.*, 1996, 1997; Richmond *et al.*, 1997a; Yang *et al.*, 1994). New information, possibly bearing important consequences for the interpretation of the PC physiopathology, was obtained in the present study by exploiting the intrinsic high propensity for the slow gating mode M2 of α subunit channels expressed in oocytes. We could, indeed, observe that the myopathic mutation studied here also produces significant changes in the kinetics and voltage dependence of mode M2 inactivation.

The effects of the mutation T1306M on the constitutively dominant mode M1, are all expected to lead per se to hyperexcitability and increased susceptibility to myotonic attacks. These effects are: (1) a slowed onset of inactivation at $V_{rel} \geq 0$ mV, that reduces the amount of inactivation during the upstroke of the action potential; (2) an acceleration of the recovery from inactivation at $V_{rel} < 0$ mV, that shortens the refractory period of the channels; and (3) a positive shift of the steady-state inactivation relative to activation curve, that increases the excitability window. Some of the effects of the mutation T1306M that we describe here for mode M2 are also in direction of increasing muscle excitability, noticeably the higher probability of this slowly inactivating mode, and the general increase of its inactivation time constant, both effects augmenting the number of channels that are practically noninactivating during action potential. Other defects are, however, of less obvious consequences on firing, most noticeably the slower recovery from M2 inactivation at $V_{rel} < 0$ mV, that might adversely by affect the hyperexcitability of M2 channels that are being frequently stimulated.

The theoretical analysis of the electrical behavior of the skeletal muscle shows that episodes of myotonic discharges and possible consequent paralysis in patients affected by sodium channelopathies may be explained by the presence of a small fraction of channels that do not inactivate (Cannon *et al.*, 1993a). We have tested, with the same analytical model, that the introduction of a relatively small fraction of channels with abnormally high P_{M2} can also lead to similar pathological effects (Moran *et al.*, 1998b, c). Furthermore, assuming the presence of channels with M1 inactivation properties modified as in a PC mutant, it is possible to obtain simulations of myotonia or paralysis episodes (Richmond *et al.*, 1997b). Whether the increase of P_{M2} or the modification of M1 inactivation is more important for the pathology of sodium channel remains to be clarified. Differences in the relative con-

tribution of these two factors might help to explain the differences in the clinical characteristics observed in patients with different mutations. A detailed description of the specific effects of each mutation on the two gating modes and on their relative probability seems, in any case, important for a better understanding the physiopathology of sodium channelopathies.

ACKNOWLEDGMENTS

We thank E. Gaggero for electronic technical assistance and M. Seri for helping in the DNA sequencing. This work is supported by Theleton, project no. 926.

REFERENCES

Auld, V. J., Goldin, A. L., Krafte, D. S., Marshall, J., Dunn, J. M., Catteral, W. A., Lester, H. A., Davidson, N., and Dunn, R. J. (1988). *Neuron* **1**, 449–61.

Barchi, R. L. (1995). *Annu. Rev. Physiol.* **57**, 355–385.

Bulman, D. E. (1997). *Hum. Mol. Genet.* **6**, 1679–1685.

Cannon, S. C. (1996). *Annu. Rev. Neurosci.* **19**, 141–164.

Cannon, S. C., Brown, R. H., and Corey, D. P. (1993a). *Biophys. J.* **65**, 270–288.

Cannon, S. C., McClatchey, A. I., and Gusella, J. F. (1993b). *Pflugers Arch.* **423**, 155–157.

Chahine, M., George, A. L., Zhou, M., Ji, S., Sun, W., Barchi, R. L., and Horn, R. (1994). *Neuron* **12**, 281–94.

Chang, S. Y., Satin, J., and Fozzart, H. A. (1996). *Biophys. J.* **70**, 2581–2592.

Cummins, T. R., and Sigworth, F. J. (1996). *Biophys. J.* **71**, 227–236.

Hamill, O., Marty, A., Neher, E., Sakmann, B., and Sigworth, F. (1981). *Pflugers Arch.* **391**, 85–100.

Hayward, L. J., Brown R. H., Jr., and Cannon, S. C. (1996). *J. Gen. Physiol.* **107**, 559–576.

Hayward, L. J., Brown, R. H., Jr., and Cannon, S. C. (1997). *Biophys. J.* **72**, 1204–1019.

Hoffman, E. P., Lehmann-Horn, F., and Rüdel, R. (1995). *Cell* **80**, 681–686.

Isom, L. L., Scheuer, T., Brownstein, A. B., Ragsdale, D. S., Murphy, B. J., and Catterall, W. A. (1995). *J. Biol. Chem.* **270**, 3306–3312.

Ji, S., Sun, W., George, A. L., Jr., Horn, R., and Barchi, R. L. (1994). *J. Gen. Physiol.* **104**, 625–643.

Ji, S., George, A. L., Horn, R., and Barchi, R. L. (1996). *J. Gen. Physiol.* **107**, 183–194.

Kudel, T. A. (1985). *Proc. Natl. Acad. Sci. U.S.* **82**, 488–492.

Liman, E. R., Tytgat, J., and Hess, P. (1992). *Neuron* **9**, 861–871.

Makita, N., Bennet, P. B., and George, A. L. (1994). *J. Biol. Chem.* **269**, 7571–7578.

Mitrovic, N., George, A. L. J., Heine, R., Wagner, S., Pika, S., Hartlaub, U., Zhou, M., and Lerche, H. (1994). *J. Physiol.* **478**, 395–402.

Mitrovic, N., Lerche, H., Heine, R., Fleischhauer, R., Pika-Hartlaub, U., Hartlaub, U., George, A. L., and Lehmann-Horn, F. (1996). *Neurosci. Lett.* **214**, 9–12.

Moorman, J. R., Kirsch, G. E., VanDongen, A. M. J., Joho, R. H., and Brown, A. M. (1990). *Neuron* **4**, 243–252.

Moran, O., Nizzari, M., and Conti, F. (1998a). In *Neuronal Circuits and Networks*: Modal Gating of Sodium Channels and Possible Physiological Implications on Hereditary Myopathies (Torre, V., and Nicolls, J., eds.), Plenum Press, New York, pp.

Moran, O., Nizzari, M., and Conti, F. (1998b). *Biophys. Biochem. Res. Commun.* **246**, 792–796.

Moran, O., Nizzari, M., and Conti, F. (1998c). *Pflugers Arch.* **435**, R16.

Patton, D. E., Isom, L. L., Catterall, W. A., and Goldin, A. L. (1994). *J. Biol. Chem.* **269**, 17640–17655.

Richmond, J. E., Featherstone, D. E., and Rube, P. C. (1997a). *J. Physiol.* **499**, 589–600.

Richmond, J. E., VanDeCarr, D., Featherstone, D. E., George, A. L. Jr., and Ruben, P. C. (1997b). *Biophys. J.* **73**, 1896–1903.

Sanger, F., Nicklen, S., and Coulson, A. R. (1977). *Proc. Natl. Acad. Sci. U.S.* **74**, MM.

Shcherbatko, A., and Brehm, P. (1998). *Biophys. J.* **74**, A397.

Stühmer, W. (1992). *Methods Enzymol.*, 319–339.

Sugimoto, M., Esaki, N., Tanaka, H., and Soda, K. (1989). *Anal. Biochem.* **179**, 309–311.

Tahmoush, A. J., Schaller, K. L., Zhang, P., Hyslop, T., Heiman-Patterson, T., and Caldwell, J. H. (1994). *Neuromusc. Disorders* **4**, 447–454.

Trimmer, J. S., Cooperman, S. S., Tomiko, S. A., Zhou, J., Crean, S. M., Boyle, M. B., Kallen, R. G., Sheng, Z., Barchi, R. L., Sigworth, F. J., Goodman, R. H., Agnew, W. S., and Mandel, G. (1989). *Neuron* **3**, 33–49.

Ukomadu, C., Zhou, J., Sigworth, F. J., and W. S., A. (1992). *Neuron* **8**, 663–676.

Wallner, M., Weigl, L., Meera, P., and Lotan, I. (1993). *FEBS Lett.* **3**, 535–539.

Wend, D. J., Starmer, C. F., and Grant, A. O. (1992). *Am. J. Physiol.* **263**, C1234–C1240.

Yang, N., Ji, S., Zhou, M., Patcek, L. J., Barchi, R. L., Horn, R., and George, A. L. J. (1994). *Proc. Natl. Acad. Sci. U. S. A* **91**, 12785–12789.

Zhou, J., Potts, J. F., Trimmer, J. S., W. S., A., and F. J., S. (1991). *Neuron* **7**, 775–785.